Optics Communications 281 (2008) 5335–5339

Contents lists available at ScienceDirect

Optics Communications

journal homepage: www.elsevier.com/locate/optcom

Slow-light enhanced light–matter interactions with applications to gas sensing

K.H. Jensen [a], M.N. Alam [b], B. Scherer [c], A. Lambrecht [c], N.A. Mortensen [d,*]

[a] Center for Fluid Dynamics, Department of Micro and Nanotechnology, Technical University of Denmark, DTU Nanotech, Building 345 East, DK-2800 Kongens Lyngby, Denmark
[b] Department of Chemical and Biochemical Engineering, Technical University of Denmark, DTU KT Building 227, DK-2800 Kongens Lyngby, Denmark
[c] Fraunhofer Institute for Physical Measurement Techniques, Heidenhofstrasse 8, D-79110 Freiburg, Germany
[d] Department of Photonics Engineering, Technical University of Denmark, DTU Fotonik, Building 345 West, DK-2800 Kongens Lyngby, Denmark

ARTICLE INFO

Article history:
Received 13 June 2008
Received in revised form 18 July 2008
Accepted 18 July 2008

PACS:
07.10.Cm
42.62.−b
42.25.Bs
42.50.Gy
42.68.Ca

ABSTRACT

Optical gas detection in microsystems is limited by the short micron scale optical path length available. Recently, the concept of slow-light enhanced absorption has been proposed as a route to compensate for the short path length in miniaturized absorption cells. We extend the previous perturbation theory to the case of a Bragg stack infiltrated by a spectrally strongly dispersive gas with a narrow and distinct absorption peak. We show that considerable signal enhancement is possible. As an example, we consider a Bragg stack consisting of PMMA infiltrated by O_2. Here, the required optical path length for visible to near-infrared detection (~760 nm) can be reduced by at least a factor of 10^2, making a path length of 1 mm feasible. By using this technique, optical gas detection can potentially be made possible in microsystems.

1. Introduction

The integration of optics and microfluidics on lab-on-a-chip microsystems has recently been the topic of much research [1–3], partly motivated by its diverse applications in chemical and biochemical analysis [4]. The miniaturization of chemical analysis systems, however, presents many optical challenges since light–matter interactions suffer from the reduced optical path length L in lab-on-a-chip systems compared to their macroscopic counterparts as illustrated in Fig. 1. Mogensen et al. [5] demonstrated that for Beer–Lambert absorption measurements in a lab-on-a-chip system, a typical size reduction by two orders of magnitude severely reduces the optical sensitivity in an inversely proportional manner. This drawback is even more pronounced for gas detection in microsystems as most gases have a very weak absorption line. Thus, microsystems may not seem the obvious solution for gas sensing and detection. On the other hand, the major reason for being interested in pursuing microsystem opportunities is of course that many applications call for compact gas sensors because of limited sensor space. On the more practical level, we emphasize that lab-on-a-chip systems can both address very minute volumes (no flow), but also allows for measurements of larger volumes flowing through the microchannels where detection takes place. In that way, spatial variations in the gas properties can potentially be mapped onto a time axis and monitored through time-traces of the optical signal. This space–time mapping is a general approach (employed for a variety of other measurements) which is only possible in microchannels supporting laminar flow. For the optical sensitivity, it has been proposed, that by introducing a porous and strongly dispersive material, such as a photonic crystal, into the lab-on-a-chip microsystems one could potentially solve these problems through slow-light enhanced light–matter interactions [6–9]. First experimental evidence of this effect for gas sensors in the mid-infrared range was reported by Lambrecht et al. [10]. Here, we extend the perturbative theory in Refs. [6–9] to the case of a dispersive Bragg stack infiltrated by a spectrally strongly dispersive gas with a narrow and distinct absorption peak. We emphasize the example of oxygen monitoring and sensing based on the two distinctive bands near the visible to near-infrared light range of 760 nm referred to as the O_2 A band [11]. Spectral data are available from the HITRAN database [12]. Though, the A band has a very weak absorption feature, it offers the potential to establish an optical in situ O_2 detection for application in many fields including combustion processes [13] and fire research [14].

2. Beer–Lambert absorption

In gas detection experiments, one typically uses Beer–Lambert absorption to determine the concentration of the substance of interest. As the light traverses the test chamber the light intensity is exponentially attenuated according to the relation

$$I = I_0 \exp(-\alpha L), \tag{1}$$

* Corresponding author. Tel.: +45 4 525 5724.
E-mail address: asger@mailaps.org (N.A. Mortensen).

0030-4018/$ - see front matter © 2008 Elsevier B.V. All rights reserved.
doi:10.1016/j.optcom.2008.07.073

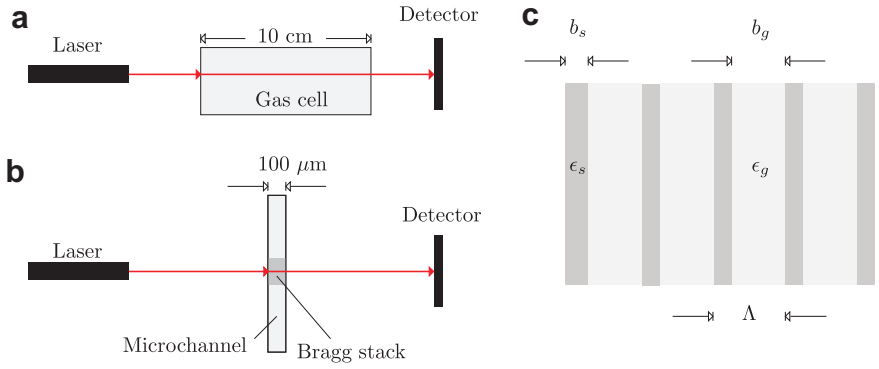

Fig. 1. (a) Schematic of a typical macroscopic gas detection setup with a light–matter interaction path length of 10 cm. (b) Schematic of a microscopic gas detection setup with a light–matter interaction path length of 100μm made possible by the presence of a Bragg stack inside the microchannel. (c) Liquid/gas infiltrated Bragg stack composed of alternating solid and gas layers of thickness b_s and b_g, respectively.

where α is the absorption coefficient, typically a linear function of the concentration $\mathscr{C}$ of absorbing molecules (not to be confused with c; the speed of light in vacuum to be introduced at a later stage). Any reduction in the optical path length L will penalize the sensitivity of the optical measurement significantly. However, by using a porous photonic crystal, it has been suggested that one may effectively enhance α by slowing down the light via a photonic crystal thereby overcoming the short path length obstacle in microsystems [6]. To quantify the enhancement, we shall use the ratio

$$\gamma = \frac{\Delta\alpha_{\mathrm{pc}}}{\alpha_{\mathrm{g}}}, \quad \Delta\alpha_{\mathrm{pc}} = \alpha_{\mathrm{pc}} - \lim_{\alpha_{\mathrm{g}}\to 0}\alpha_{\mathrm{pc}}, \tag{2}$$

where α_{pc} is the absorption coefficient inside the photonic crystal and α_{g} the corresponding homogeneous space absorption coefficient associated with the gas itself. The subscripts are introduced in order to carefully distinguish between absorption taking place in the photonic crystal material and the gas, respectively. In this work we consider the particular simple one-dimensional example of a Bragg stack and extend previous work [15] by using a more realistic model for the gas absorption profile.

3. The Bragg stack

The periodic Bragg stack is illustrated in panel (c) of Fig. 1 and is composed of alternating layers of gas and solid of thickness b_{g} and b_{s}, respectively. The lattice constant is $\Lambda = b_{\mathrm{g}} + b_{\mathrm{s}}$ and for the dielectric functions we allow for complex-valued bulk parameters, i.e. $\epsilon_{\mathrm{g}} = \epsilon'_{\mathrm{g}} + \mathrm{i}\epsilon''_{\mathrm{g}}$ and $\epsilon_{\mathrm{s}} = \epsilon'_{\mathrm{s}} + \mathrm{i}\epsilon''_{\mathrm{s}}$. For later convenience we rewrite the dielectric functions in terms of the bulk refractive index n and the damping coefficient α,

$$\epsilon_{\mathrm{g}} = n_{\mathrm{g}}^2 + \mathrm{i}n_{\mathrm{g}}\alpha_{\mathrm{g}}/k, \tag{3a}$$

$$\epsilon_{\mathrm{s}} = n_{\mathrm{s}}^2 + \mathrm{i}n_{\mathrm{s}}\alpha_{\mathrm{s}}/k, \tag{3b}$$

where $k = 2\pi/\lambda = \omega/c$ is the free-space wave vector with λ being the corresponding free-space wavelength and ω the angular frequency. The dispersion relation for the Bragg stack is governed by (see Ref. [15] and references therein)

$$\cos(\kappa\Lambda) = F(k), \tag{4a}$$

where κ is the Bloch wave vector and

$$F(k) = \cos\left(\sqrt{\epsilon_{\mathrm{g}}}kb_{\mathrm{g}}\right)\cos\left(\sqrt{\epsilon_{\mathrm{s}}}kb_{\mathrm{s}}\right) - \frac{\epsilon_{\mathrm{g}}+\epsilon_{\mathrm{s}}}{2\sqrt{\epsilon_{\mathrm{g}}\epsilon_{\mathrm{s}}}} \times \sin\left(\sqrt{\epsilon_{\mathrm{g}}}kb_{\mathrm{g}}\right)\sin\left(\sqrt{\epsilon_{\mathrm{s}}}kb_{\mathrm{s}}\right). \tag{4b}$$

In the following we explicitly write the Bloch wave vector as $\kappa \equiv \kappa' + \mathrm{i}\kappa''$, where κ' and κ'' are real and imaginary parts, respectively. The imaginary part causes an exponential damping of the Bloch states with a corresponding attenuation coefficient $\alpha_{\mathrm{pc}} = 2\kappa''$. Likewise, in the homogeneous case we have $\alpha_{\mathrm{g}} = k\epsilon''_{\mathrm{g}}/\sqrt{\epsilon'_{\mathrm{g}}}$ and in this way Eq. (2) now becomes

$$\gamma = \frac{2\sqrt{\epsilon'_{\mathrm{g}}}}{\epsilon''_{\mathrm{g}}} \times \frac{\kappa''(\epsilon''_{\mathrm{s}}, \epsilon''_{\mathrm{g}}) - \kappa''(\epsilon''_{\mathrm{s}}, \epsilon''_{\mathrm{g}} \to 0)}{k}. \tag{5}$$

If γ is greater than unity, it means that we have enhanced absorption due to the geometry of the Bragg stack. The absorption enhancement comes about because the group velocity of the light $\partial\omega/\partial\kappa'$ is reduced by the geometry of the Bragg stack [6]. In Eq. (5), the slow light phenomenon manifests itself through an increasing imaginary part of the Bloch vector κ'' as the band edge is approached. In deriving Eq. (5), we have separated the two different contributions to the absorption from the gas and the solid, thus implicitly assuming a small change in attenuation caused by the presence of the gas. However, we emphasize that the effect of material dispersion is included in the dispersion relation in an exact analytical and non-perturbative way and thus our results fulfill the Kramers–Kronig relation by taking the full interplay between waveguide and material dispersion into account.

4. Examples

In the following we illustrate the prospects for slow-light enhanced absorption by means of examples.

4.1. Non-absorbing materials

First, we consider the problem of two non-absorbing materials, say a gas and a polymer with $\epsilon_{\mathrm{g}} = 1.0^2$ and $\epsilon_{\mathrm{s}} = 1.5^2$. The corresponding band diagram, obtained from a numerical solution of Eq. (4a), is shown in Fig. 2. Two band gaps, indicated by yellow shading, are visible near $\omega\Lambda/c = 2.8$ and 5.5. As can be seen, the group velocity approaches zero near the band gap edges while the imaginary part of κ attains a finite value only inside the band gaps where propagation of electromagnetic radiation is prohibited due to the exponential damping.

4.2. Frequency-independent weakly absorbing materials

Next, we consider two weakly absorbing materials, say again the same gas and polymer, but now with imaginary contributions to the dielectric functions corresponding to damping parameters $\alpha_{\mathrm{g}}\Lambda = \alpha_{\mathrm{s}}\Lambda = 0.1$. As seen from the corresponding band diagram in Fig. 3, the main cause is to smear out the spectrally pronounced